11-16-2016

Improving global detection of volcanic eruptions using the Ozone Monitoring Instrument (OMI)

Verity Flower
Michigan Technological University, vjflower@mtu.edu

Thomas Oommen
Michigan Technological University, toommen@mtu.edu

Simon Carn
Michigan Technological University, scarn@mtu.edu

Recommended Citation

Flower, V., Oommen, T., & Carn, S. (2016). Improving global detection of volcanic eruptions using the Ozone Monitoring Instrument (OMI). *Atmospheric Measurement Techniques, 9*(11), 5487-5498. http://doi.org/10.5194/amt-9-5487-2016
Retrieved from: https://digitalcommons.mtu.edu/michigantech-p/3183

Follow this and additional works at: https://digitalcommons.mtu.edu/michigantech-p

 Part of the Geological Engineering Commons, and the Mining Engineering Commons

Atmos. Meas. Tech., 9, 5487–5498, 2016
www.atmos-meas-tech.net/9/5487/2016/
doi:10.5194/amt-9-5487-2016

Atmospheric Measurement Techniques
Open Access
EGU

Improving global detection of volcanic eruptions using the Ozone Monitoring Instrument (OMI)

Verity J. B. Flower, Thomas Oommen, and Simon A. Carn

Dept. Geological and Mining Engineering and Sciences, Michigan Technological University, 1400 Townsend Dr, Houghton, MI 49931, USA

Correspondence to: Verity J. B. Flower (vjbflower@gmail.com)

Received: 14 June 2016 – Published in Atmos. Meas. Tech. Discuss.: 4 July 2016
Revised: 29 October 2016 – Accepted: 31 October 2016 – Published: 16 November 2016

Abstract. Volcanic eruptions pose an ever-present threat to human populations around the globe, but many active volcanoes remain poorly monitored. In regions where ground-based monitoring is present the effects of volcanic eruptions can be moderated through observational alerts to both local populations and service providers, such as air traffic control. However, in regions where volcano monitoring is limited satellite-based remote sensing provides a global data source that can be utilised to provide near-real-time identification of volcanic activity. This paper details a volcanic plume detection method capable of identifying smaller eruptions than is currently feasible, which could potentially be incorporated into automated volcanic alert systems. This method utilises daily, global observations of sulfur dioxide (SO_2) by the Ozone Monitoring Instrument (OMI) on NASA's Aura satellite. Following identification and classification of known volcanic eruptions in 2005–2009, the OMI SO_2 data, analysed using a logistic regression analysis, permitted the correct classification of volcanic events with an overall accuracy of over 80 %. Accurate volcanic plume identification was possible when lower-tropospheric SO_2 loading exceeded ~ 400 t. The accuracy and minimal user input requirements of the developed procedure provide a basis for incorporation into automated SO_2 alert systems.

1 Introduction

Volcanic eruptions pose a global hazard due to the potential for emissions to be entrained into the upper atmosphere and transported globally. Emissions from volcanoes can have significant impacts on human health (Delmelle et al., 2002; Hansell and Oppenheimer, 2004), on the aviation industry (Miller and Casadevall, 1999; Prata, 2009), and on atmospheric radiative transfer as seen following the eruption of Mt Pinatubo (Self et al., 1993). In order to mitigate the possible impacts of volcanic eruptions, timely warning of events is essential. Since the installation of a global network of ground-based monitoring stations is both costly and impractical, satellite-based remote sensing data are currently used to provide the spatial and temporal coverage necessary for near-real-time (NRT) monitoring of volcanic eruption clouds (Brenot et al., 2014). Existing volcanic cloud detection techniques employ a threshold approach to identify volcanic eruptions, but this can limit their capabilities with respect to smaller events. The following work outlines a method to distinguish smaller volcanic plumes through the implementation of a background correction factor. The Ozone Monitoring Instrument (OMI), launched on NASA's Aura satellite in July 2004, provides near-global daily monitoring of multiple atmospheric trace gases with absorption features in the ultraviolet (UV) spectral band. OMI was designed to supersede the Total Ozone Monitoring Spectrometer (TOMS) instrument and provide higher-spatial-resolution data than were previously available. Strong absorption bands in the UV allow sulfur dioxide (SO_2) to be discerned by instruments designed to measure ozone (Krueger, 1983). The capability of satellite-based volcanic SO_2 detection was first demonstrated following the eruption of El Chichón in 1982 (Krueger, 1983), leading to the implementation of satellite-based UV measurements as a volcano monitoring tool (Schneider et al., 1999; Krueger et al., 2008; Carn et al., 2016). The low spatial resolution of the TOMS instruments precluded the measurement of SO_2 in small volcanic eruptions (Carn et al., 2003). OMI's

higher spatial resolution (13×24 km at nadir) permits detection of smaller eruptions and passive volcanic degassing of SO_2, whilst providing daily, global coverage (Krotkov et al., 2006; Carn et al., 2013, 2016). This work utilises the continuous global coverage of OMI to identify and automatically classify volcanic eruptions based on common characteristics established through the use of statistical modelling.

Existing alert systems

The Support to Aviation Control Service (SACS) is one operational alert system currently used to detect SO_2 and ash emitted from volcanoes (Brenot et al., 2012). This service provides NRT alerts of anomalously high SO_2 amounts and ash indices recorded by four UV instruments: OMI, the Global Ozone Monitoring Experiment-2 (GOME-2; flown on board two meteorological satellites: MetOp-A and MetOp-B), and the Ozone Mapping and Profiler Suite (OMPS). Three infrared (IR) instruments are also used: the Atmospheric Infrared Sounder (AIRS) and Infrared Atmospheric Sounding Interferometer (IASI; also flown on the MetOp-A and -B platforms). The method of SO_2 alert generation used by SACS (Brenot et al., 2014; http://sacs.aeronomie.be/info/index.php) involves the initial identification of an anomalously high SO_2 column amount (> 2 DU). When a pixel is flagged, the area is analysed in greater detail, and an alert is only generated if more than half of the neighbouring pixels also display high SO_2 values (> 2 DU). The technique developed by Brenot et al. (2014) is subject to certain limitations when utilising UV data, including the systematic noise in the data leading to false alerts and the restriction of retrievals to those that assume a SO_2 plume altitude in the lower stratosphere (STL). Therefore, in the development of an algorithm based on OMI data we aim to account for variable background SO_2 levels and systematic noise. Additionally, SO_2 retrievals representing a lower plume altitude are used, in an attempt to resolve plumes with lower SO_2 amounts, lower injection altitude, and more diffuse characteristics.

2 Methodology

To distinguish volcanic events from background SO_2 levels, the characteristics of volcanic emissions must be assessed. In this work we implement statistical classification techniques such as logistic regression to isolate observed variations in volcanic SO_2 plumes compared to ambient SO_2 levels. The use of statistical modelling also facilitates the review of misclassified events, providing some insight into the limitations of the detection algorithm. The aim of this work is to distinguish volcanic events from control samples with a binary classification algorithm and identify the strengths and weaknesses of the resulting methodology. To develop a model and identify characteristics specific to volcanic plumes, three datasets must be compiled. Firstly, a database of emissions corresponding to known volcanic eruptions must be obtained, with a complimentary dataset incorporating measurements collected during known inactive periods against which to compare volcanic events. These two elements are used to train the statistical models developed and establish whether volcanic events can be distinguished from non-volcanic ones. The final dataset is a collection of volcanic and non-volcanic events not used to train the original model, against which the efficacy of the model can be tested. The following section details the data collection and statistical applications used.

2.1 Satellite data

For this analysis we use OMI Level 2 total column SO_2 (OMSO2) data, which are publicly available from NASA Goddard Earth Sciences (GES) Data and Information Services Center (DISC; http://disc.sci.gsfc.nasa.gov/Aura/data-holdings/OMI/omso2_v003.shtml). These data provide global coverage with a temporal resolution of 1 day at low latitudes and increasing daily observations towards the poles, where measurement swaths overlap. Until June 2016, OMSO2 data provided volcanic SO_2 total column amounts calculated using a linear fit (LF) algorithm (Yang et al., 2007), which are the products used here. Previous works have provided in-depth descriptions of the OMI retrieval algorithms (Carn et al., 2013; Krotkov et al., 2006; McCormick et al., 2013; Yang et al., 2007), which have a proven track record in the assessment of volcanic and anthropogenic emissions, including identification of volcanic plume sources (e.g. Carn et al., 2008, 2013, 2016; McCormick et al., 2012, 2013), volcanic plume tracking (e.g. Carn and Prata 2010; Krotkov et al., 2010; Lopez et al., 2013), and identification of copper smelter emissions (Carn et al., 2007) and other large SO_2 emission sources (e.g. Fioletov et al., 2011, 2013).

The LF algorithm retrieves three SO_2 column amounts corresponding to a priori SO_2 vertical profiles with centre of mass altitudes (CMAs) of approximately 3 km (lower troposphere; TRL), 8 km (mid-troposphere; TRM), and 17 km (STL). These altitudes are based upon atmospheric pressure levels and therefore can display slight variations depending upon the local temperature profile (Carn et al., 2013). In order to obtain an accurate estimation of the SO_2 column amount, the appropriate SO_2 retrieval must be selected based upon the known or inferred injection altitude of the volcanic plume (Yang et al., 2007), which can be poorly constrained particularly in remote regions with minimal or no monitoring capabilities. Differences between the altitude assumed in the LF algorithm and the true altitude of the plume can lead to errors of up to 20 %, provided the assumption is approximately correct (Yang et al., 2007). Since our aim is to develop an algorithm capable of detecting volcanic eruptions regardless of magnitude, including diffuse SO_2 clouds, we use the TRL SO_2 product to permit identification of small eruptions confined to the lower troposphere. The use of one retrieval altitude reduces the need for user input or prior knowledge of the injection altitude of the plume but will result in the

Table 1. Characteristics of the methods incorporated in the development of an automatic classification technique.

Method	Sample area size	Position	Correction technique
M_1	$4° \times 4°$	Centred over the volcano	None applied
M_2	$2° \times 2°$	Centred over the volcano	None applied
M_3	$2° \times 2°$	Centred over the volcano	Assumes that the plume is predominantly confined to the M_2 region and utilises the M_1 region to define the background SO_2 level (Eq. 1)

overestimation of SO_2 mass for plumes injected into the mid-troposphere or above. This method is hence sufficient for plume identification and alert purposes but precludes accurate plume mass calculation for some eruptions. SO_2 retrievals corresponding to higher altitudes (TRM or STL) not only feature lower background noise but also significantly underestimate SO_2 columns in low-altitude volcanic clouds, possibly preventing detection.

OMI data collected since 2008 are influenced by a row anomaly (the OMI row anomaly; ORA) which results in data gaps in particular rows along the OMI measurement swath. Information on the status of this anomaly is provided by the Royal Netherlands Meteorological Institute (http://projects.knmi.nl/omi/research/product/rowanomaly-background.php). The ORA data gaps combined with the variation in viewing angle produced by the 16-day orbital cycle of the Aura satellite result in varying influence on OMI SO_2 measurements (Flower et al., 2016). Any eruptions identified after the appearance of the ORA were investigated with greater scrutiny and excluded where the effect was significant.

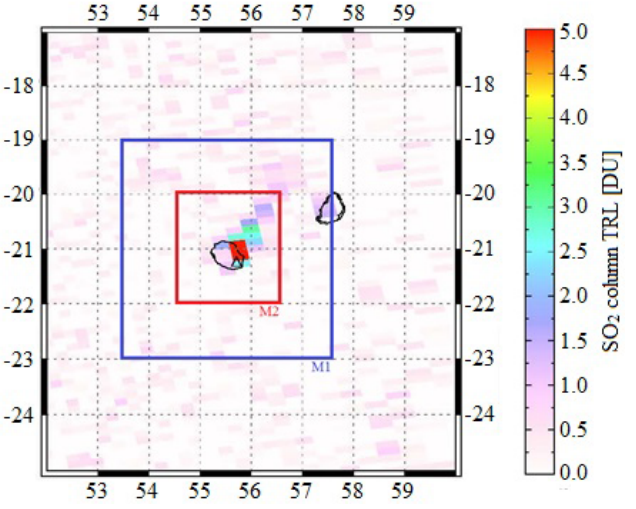

Figure 1. Analysis regions for method 1 (M_1) and method 2 (M_2) for an SO_2 plume detected by OMI at Piton de la Fournaise, Réunion, on 24 February 2010.

2.2 Volcanic plume quantification

As a training dataset for our plume identification technique, we identified 79 volcanic eruptions at 27 different volcanoes (Table 1) using the Volcanoes of the World (VOTW) database curated by the Smithsonian Institution's Global Volcanism Program (GVP; see Global Volcanism Program, 2013). Note that, as a result of the way in which eruptions are defined in the VOTW database, several of the eruptions listed in Table 1 actually correspond to the onset of extended periods of volcanic activity, rather than discrete eruptions. For each identified eruption, total SO_2 mass detected by OMI was obtained for the registered day of the eruptive event (or the start of the period of unrest) with the preceding and subsequent days analysed where no corresponding plume could be identified on the reported day of eruption. This allowance accounts for any inaccuracies in the assigned eruption date and allows for the identification of eruption plumes generated after the Aura overpass time ($\sim$ 13:45 local time) resulting in a delay in detection. Identification and quantification of volcanic SO_2 emissions is complicated by the presence of variable biases and noise levels in the data. These variations are influenced by several factors, including the latitude of the volcano, time of year, proximity to pollution sources, and the presence of meteorological clouds (Krotkov et al., 2006; Yang et al., 2007).

In our analysis, three methods (M_1, M_2, and M_3; Table 1) were used to quantify the SO_2 loading detected at each location, with the goal of distinguishing volcanic SO_2 from background noise. The procedures were developed with the intention of allowing the calculation of volcanic SO_2 loading with minimal user input, reducing the possible effects of human error in the classification of what constitutes the bounds of an identified plume.

Method 1 (M_1) and method 2 (M_2) differ only in the geographic extent over which OMI SO_2 columns are integrated to obtain total SO_2 mass (Fig. 1). For each eruption analysed, M_1 calculates integrated SO_2 mass in a $4° \times 4°$ box centred over the volcano location (thus capturing plumes regardless of wind direction). The $4° \times 4°$ box encompasses an area which captures most small–moderate volcanic plumes with few instances of dispersion of emissions outside the region; however, this relatively large sample area also potentially includes greater background noise, particularly where other

nearby volcanoes are also active. Regions with increased background SO_2 concentrations from multiple sources would result in a higher number of false alerts. As an alternative to M_1, M_2 uses a $2° \times 2°$ region which, whilst more susceptible to possible plume dispersion beyond the defined limits, is less influenced by contamination (Fig. 1). Manual inspection indicated that plume dispersion beyond the defined geographic limits was only an issue for the largest eruptions in Table 2. Figure 1 shows an example of a small volcanic SO_2 plume at Piton de la Fournaise volcano (Réunion); here, the M_2 region captures most of the SO_2 plume that is visually apparent, only excluding some very diffuse SO_2 further downwind that is included in the M_1 region.

A third method (M_3) was developed in an attempt to intrinsically account for the variable noise levels in SO_2 data collected in different geographic regions (Carn et al., 2013). We posit that in order to effectively develop a global volcanic plume detection methodology without a significant number of false alerts a background noise correction may be necessary. Our technique is analogous to contextual thermal infrared (TIR) anomaly detection procedures used at active volcanoes, where a background radiance value is calculated as a reference against which anomalously high radiance values can be compared (e.g. Wright et al., 2002; Murphy et al., 2011). In the M_3 method, the $2° \times 2°$ region (M_2) is considered the active emission region with a background SO_2 offset value derived from the total SO_2 mass in the $4° \times 4°$ M_1 region (Eq. 1).

$$M_3 = M_2 - \frac{M_1 - M_2}{3} \quad (1)$$

Classification based on a latitudinal range leads to variations in the physical dimensions of the analysis region depending upon the latitude of the volcano. The maximum such variation in this analysis would occur between equatorial volcanoes and those located in Kamchatka and Alaska, equating to 2.8 and 1.4 km in the north–south dimensions of the M_1 and M_2 regions respectively. This equates to the loss of less than one pixel at the furthest extent of the analysis region and is not likely to influence the resulting analyses. In contrast the variation in the longitudinal dimensions equates to a $\sim 35\,\%$ decrease in the east–west dimensions of high-latitude regions relative to the Equator. The high-latitude samples analysed here will be investigated to identify whether this variation in sample size influenced the sample classification techniques employed.

Eruptive events that post-date the appearance of the ORA were manually assessed in order to identify whether the ORA data gap significantly impacted the detection of SO_2, such as complete masking of the plume in extreme cases (Flower et al., 2016). Additional factors impacting the selection of eruptive events are the presence of meteorological clouds, which can effectively mask any volcanic plume at lower altitudes from a satellite-based sensor (Carn et al., 2013; Krotkov et al., 2006), and the seasonal variation in UV radiation at high

Table 2. Test dataset of volcanic eruption dates and control dates (organised alphabetically by volcano).

Volcano	Location	Eruption date	Control date
Ambrym	Vanuatu	08/11/2006	31/03/2005
		23/05/2008	04/06/2008
Anatahan	Mariana Islands	06/01/2005	11/05/2009
		05/04/2005	16/06/2006
		17/03/2006	15/01/2007
		24/02/2007	22/11/2005
		27/11/2007	29/06/2005
Bagana	Papua New Guinea	17/03/2005	26/11/2007
		06/06/2005	14/06/2008
		09/01/2007	25/04/2005
		10/03/2007	23/10/2006
		20/05/2007	06/11/2006
		14/07/2007	01/07/2009
		23/08/2007	22/01/2006
		12/09/2007	26/12/2009
		06/10/2007	01/03/2009
Bezymianny	Kamchatka, Russia	10/05/2007	31/01/2005
		11/07/2008	22/05/2008
Chaitén	Chile	02/05/2008	11/12/2009
Dukono	Indonesia	25/05/2008	03/03/2006
		25/07/2008	02/10/2008
Fuego	Guatemala	27/12/2005	03/04/2008
Ibu	Indonesia	04/04/2008	16/07/2008
Kathala	Comoros	16/04/2005	07/07/2005
		24/11/2005	12/09/2006
		28/05/2006	17/10/2008
		12/01/2007	24/05/2009
Kelut	Indonesia	18/05/2006	21/02/2006
Manam	Papua New Guinea	27/01/2005	15/07/2005
		17/07/2006	25/02/2005
		05/10/2007	24/11/2008
		29/12/2007	07/08/2005
		11/05/2008	04/07/2008
Mayon	Philippines	17/08/2005	02/08/2006
		21/02/2006	27/03/2008
Merapi	Indonesia	07/03/2006	29/05/2008
		11/03/2006	31/03/2007
Nyamuragira	DR Congo	27/11/2006	09/12/2007
		02/01/2010	11/05/2009
		06/11/2011	03/09/2008
		22/06/2014	31/08/2008
Nyiragongo	DR Congo	07/09/2005	22/06/2006
		10/10/2005	27/08/2005
		07/11/2005	08/03/2007
		01/01/2009	09/05/2009

Table 2. Continued.

Volcano	Location	Eruption date	Control date
Ol Doinyo Lengai	Tanzania	20/07/2005 30/03/2006	20/07/2005 11/03/2008
Pagan	Mariana Islands	11/01/2007	24/06/2007
Piton de la Fournaise	Réunion	24/02/2005 20/07/2006 30/08/2006	01/02/2006 22/03/2007 13/11/2008
Popocatépetl	Mexico	06/04/2006 23/05/2006 11/04/2007 01/12/2007 22/02/2008 16/11/2008	22/02/2006 27/08/2005 08/03/2007 09/05/2009 25/02/2005 11/03/2008
Rabaul	Papua New Guinea	07/10/2006 04/08/2007 22/08/2007	24/06/2007 01/02/2006 22/03/2007
Santa Ana	El Salvador	01/10/2005	13/11/2008
Santa Maria	Guatemala	26/10/2005	22/02/2006
SHV	Montserrat	20/05/2006 08/01/2007 29/07/2008 11/02/2010	10/04/2009 12/03/2008 05/06/2007 02/04/2007
Soputan	Indonesia	19/04/2005 15/12/2006 15/12/2006 06/06/2008	07/02/2005 10/05/2009 17/11/2008 20/12/2006
Tinakula	Solomon Islands	12/02/2006 22/09/2009 17/01/2010	03/02/2009 15/06/2009 05/10/2005
Tungurahua	Ecuador	14/07/2006 16/08/2006 10/01/2008 06/02/2008	16/06/2005 31/12/2009 04/05/2009 11/02/2007
Turrialba	Costa Rica	06/01/2010 12/01/2012	06/09/2005 04/08/2005

Dates are displayed as DD/MM/YYY.

latitudes. Cloud masking is due to the high UV albedo of clouds, and this, coupled with low UV irradiance, can make SO_2 detection at high latitudes during winter months particularly challenging (Telling et al., 2015). Through implementation of a cloud fraction threshold of ~ 20 % within each scene the majority of the eruptions analysed here were restricted to latitudes below 30°.

2.3 Control samples

A control group is required to assess whether volcanic eruptions can be distinguished from background SO_2 levels. Therefore, for each volcanic eruption analysed (Table 2) a control SO_2 mass was calculated using each of the three incorporated methodologies (M_1, M_2, and M_3) for a second date at the same volcano. Assignment of control group analysis dates was limited to a period between 1 January 2005 and 31 December 2009. The 2009 cut-off date was employed due to the increasing influence of the ORA after this time, in an attempt to reduce the influence of data gaps on the model output. Control dates were assigned for comparison with each identified volcanic eruption, using an online random-number generator (Haahr, 2015; http://www.random.org) to assign a value between 0 and 1825 to each data point. These random values were used to determine the number days from the beginning of the analysis period at which to assign a control date (Table 2). The identified dates were then assigned to each target volcano alphabetically, with a corresponding number of events assigned to each location as number of volcanic eruption analyses performed (Table 2).

2.4 Modelling techniques

Modelling procedures were conducted with the Weka 3 software package: a collection of algorithms that can be implemented for data mining tasks (Hall et al., 2009) provided by the University of Waikato (http://www.cs.waikato.ac.nz/ml/weka/). The quantity of SO_2 present within each analysis region is a complex function of eruption composition and magnitude in addition to ambient SO_2 levels and local sources of interference such as neighbouring volcanoes. This precludes the use of a fixed threshold, whereas statistical models permit a probabilistic approach to volcanic eruption identification with multiple statistical analyses trialled using the Weka 3 package. A simple logistic regression analysis (Eq. 2) was found to be the most effective technique for the classification of volcanic and non-volcanic events. Simple logistic regression is a binary classification technique, here defining volcanic (v) and non-volcanic control (c) events and facilitating the development of a linear model constructed from a transformed target variable (Witten and Frank, 2005). The logistic regression equation used here assigns the probability P of the occurrence of a volcanic eruption or degassing event:

$$P = 1 - \frac{1}{1 + e^{-(a+bX)}}, \quad (2)$$

where e is the base of the natural logarithm, a is the probability when the independent variable (X; here, the volcanic plume SO_2 mass measured is in tonnes) is equal to 0, and b represents the rate at which probabilities vary with incremental changes in X.

Output of a logistic regression analysis is assessed against a series of validation statistics that test the accuracy of the

generated model. These statistics include overall accuracy, precision, and recall, in addition to receiver operating characteristic (ROC) curves. In this analysis, the overall accuracy relates to the percentage of correctly classified events in both the volcanic and control (non-volcanic) samples; however, this statistic alone cannot account for preferential classification of one sample over another (Oommen et al., 2010). Hence precision and recall statistics, characterised by values between 0 and 1, are used to identify whether preferential classification is occurring. Precision relates to the accuracy of prediction of a single sample group (volcanic or non-volcanic), whilst recall measures the effectiveness of the predictions themselves (Oommen et al., 2010). In the context of this study, if a volcanic classification has a precision of 0.9, then 90 % of the events predicted as being volcanic in nature are volcanic events, whilst the remaining 10 % are misclassified as non-volcanic and will be termed here as "missed alerts". In contrast, a recall value of 0.8 would correspond to 80 % of observed volcanic events being correctly classified, but this does not take into account any non-volcanic events which are misclassified as volcanic, referred to here as "false alerts". The final validation statistic used here is the ROC curve, which represents a method for assessing the rate of accurately classified events against possible falsely classified events. ROC values relate to the accuracy of the classification system implemented, with a value of 1 indicating accurate prediction of all events (Oommen et al., 2010; Witten and Frank, 2005).

Logistic regression model calculation was conducted using the k-fold cross-validation technique incorporated into the Weka 3 software package. This method segregates the data into k partitions, allowing k-1 segments of the data to be used as a training set, with the remaining data used for validation purposes. This method is then repeated with each of the k partitions being used to validate the corresponding model from which it was withheld, with the final statistics comprising an average of the output of all k models (Oommen et al., 2010). We implement a k value of 10 due to the associated reduction in bias compared to k values < 5 (Rodríguez et al., 2010; Witten and Frank, 2005).

3 Results

Of the three SO_2 mass calculation procedures employed (M_1, M_2, and M_3), the most success was achieved with the background-corrected dataset (M_3). None of the logistic regression model investigations undertaken with the M_1 and M_2 datasets produced more than 55 % overall accuracy in the classification of volcanic events, and therefore these data were not investigated further. In contrast, the M_3 technique provided the best results, with a 77 % overall accuracy and no additional data pre-processing required; therefore this technique was employed for all further assessments and model development.

Table 3. Average SO_2 column amounts (tonnes) for volcanic and control events.

Sample		Average SO_2 mass (tonnes)
Volcanic	M_1 (4°)	2680
	M_2 (2°)	1150
	M_3 (corrected)	680
Control	M_1 (4°)	450
	M_2 (2°)	170
	M_3 (corrected)	90

3.1 OMI SO_2 measurements

Of the 79 volcanic eruptions analysed, 13 displayed low SO_2 amounts (< 100 t), following application of the SO_2 correction (M_3), on the identified day of eruption. Two eruptions produced very large amounts of SO_2: Nyamuragira (November 2006; 46 kt) and Rabaul (October 2006; 550 kt); however, use of the OMI TRL SO_2 columns is likely to overestimate the actual SO_2 amounts in these upper-tropospheric or lower-stratospheric plumes (Carn et al., 2013).

Excluding the aforementioned very high values, the average M_3 plume contained 680 t of SO_2, approximately 60 % of the average of the M_2 analysis and 25 % of the M_1 average (Table 3). The control dataset displays significantly lower SO_2 loadings than the volcanic events, with an average corrected SO_2 mass of 90 t and a maximum corrected SO_2 mass of 1040 t. This variation indicates that the volcanic data displays generally higher SO_2 levels than the control data, as would be expected. In all of the selection methodologies the SO_2 mass detected on control dates was 14–17 % of the average mass detected in the volcanic dataset. Box plots were generated to assess the general dynamics of the volcanic and control datasets (Fig. 2). Comparison of these plots confirms the pattern identified in Table 3, with the SO_2 measurements on "eruption" days displaying significantly higher values than the control data.

3.2 Model output

The most accurate model consisted of a simple logistic regression applied to the M_3 SO_2 dataset with an overall accuracy of 76.6 % and an ROC of 0.843. This model favoured volcanic precision (volcanic precision of 0.83 vs. control precision of 0.72) at the expense of control recall (control recall of 0.86 vs. volcanic recall of 0.67), which indicates that the model preferentially classifies alerts as control samples. This model reduces the number of false alerts generated relative to missed alerts. Investigations were undertaken to identify characteristics of volcanic events that facilitated classification and to elucidate the likely cause of the 23 % error associated with the model. Removal of volcanic plumes containing less than 50 t of SO_2 from the M_3 dataset resulted in

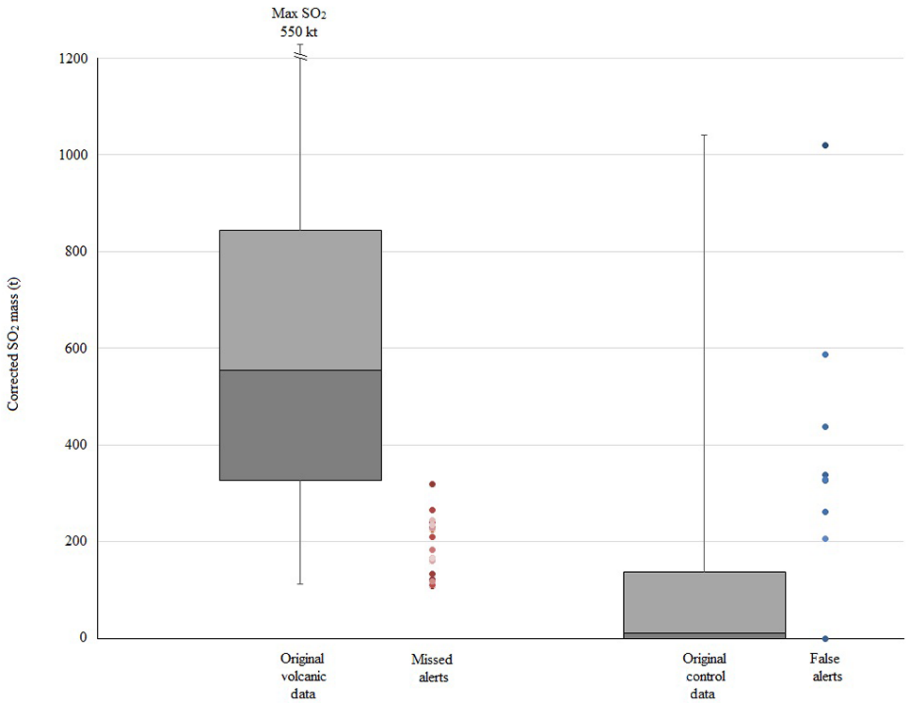

Figure 2. Box-and-whisker plots displaying the spread and distribution of volcanic and control data, with lines indicating upper and lower quartiles of the data and the remainder represented by the box region. Additional data points indicate the individual missed alerts in the volcanic data and false alerts in the control data detailed in Table 4.

a $\sim 6\,\%$ increase in model accuracy. Eight data points produced false alerts with control events classified as volcanic eruptions, whilst 18 volcanic events were misclassified as controls, producing missed alerts (Table 4). The misclassified alerts were isolated to assess if any common characteristics of these events could be identified, with each individual alert incorporated into Fig. 2 for comparison with the overall dynamics of the data. The comparison of missed alerts indicates that each one falls within the lower quartile of the volcanic dataset, whilst the false alerts displayed values consistent with the upper quartile of the control data range (with one exception; see Fig. 2). The potential causes of the misclassification of events are discussed further in Sect. 4.1.

4 Discussion

4.1 Analysis of inaccurate classifications

4.1.1 False alerts

Investigation of the incorrectly classified false alerts (Fig. 2; Table 4) revealed that, due to the random selection procedure used for assigning control sample dates, some of the control SO_2 values corresponded to periods of ongoing volcanic activity. These anomalous control values relate to stronger, persistent plumes, despite not being associated with large or "initiating" events as reported in the VOTW database; this was the case for five of the nine false alerts (C1, 8, 32, 54, and 57; Table 4). Two additional alerts were generated as a result of a data gap in the OMI measurements (C10 and 24). Missing values (characterised by a blank cell to differentiate these from days with data available but no recordable SO_2 emissions) are incorrectly classified by the incorporated model as volcanic events. Pre-screening of samples for data gaps prior to incorporation into the model is required to prevent the classification of missing values as volcanic events. The one remaining false alert (C29) was the result of increased noise levels preferentially affecting the M_2 over the M_1 region, resulting in an artificially high SO_2 mass derived from the M_3 calculation and a false alert.

4.1.2 Missed alerts

Missed alerts occurred at a higher frequency than false alerts, but a common characteristic of all missed alerts is an SO_2 plume mass below 325 t (Fig. 2; Table 4). We attribute the misclassification of volcanic events to four main causes. The first influenced eight of the volcanic events (V3, 13, 20, 23, 28, 32, 33, and 48; Table 4) and is the result of eruptions producing diffuse plumes containing low SO_2 amounts close to the OMI detection limit (e.g. small eruptions and/or eruptions to low altitudes). The second cause of misclassification affecting eight samples (V5, 17, 21, 24, 34, 43, 64, and 67; Table 4) is the drifting of the volcanic plume out of the geographic area of analysis (M_2) into the region utilised for background classification (M_1), causing signal suppres-

Table 4. Misclassified alerts identified in the initial logistic regression model.

Sample (S)		Name	Date (DD/MM/YYYY)	Plume SO_2 mass (tonnes)	Predicted classification	Original classification	Error generation
C	1	Ambrym	31/03/2005	1040	Volcanic	Control	Persistent degassing
C	8	Bagana	26/11/2007	340	Volcanic	Control	Persistent degassing
C	10	Bagana	23/10/2006	?	Volcanic	Control	Missing data
C	24	Karthala	07/07/2005	?	Volcanic	Control	Missing data
C	29	Manam	15/07/2005	350	Volcanic	Control	Localised noise
C	32	Manam	07/08/2005	450	Volcanic	Control	Small Eruption
C	54	Popocatépetl	08/03/2007	600	Volcanic	Control	Ongoing eruption
C	57	Popocatépetl	11/03/2008	340	Volcanic	Control	Ongoing eruption
V	3	Anatahan	06/01/2005	230	Control	Volcanic	Diffuse plume
V	5	Anatahan	17/03/2006	120	Control	Volcanic	Drifting plume
V	13	Bagana	14/07/2007	320	Control	Volcanic	Diffuse plume
V	17	Bezymianny	10/05/2007	140	Control	Volcanic	Drifting plume
V	19	Chaiten	02/05/2008	250	Control	Volcanic	High noise
V	20	Dukono	25/05/2008	300	Control	Volcanic	Diffuse plume
V	21	Dukono	25/07/2008	270	Control	Volcanic	Drifting plume
V	23	Ibu	04/04/2008	210	Control	Volcanic	Diffuse plume
V	24	Karthala	16/04/2005	110	Control	Volcanic	Drifting plume
V	28	Kelut	18/05/2006	170	Control	Volcanic	Diffuse plume
V	32	Manam	29/12/2007	80	Control	Volcanic	Diffuse plume
V	33	Manam	11/05/2008	190	Control	Volcanic	Diffuse plume
V	34	Mayon	17/08/2005	120	Control	Volcanic	Drifting plume
V	43	Nyiragongo	10/10/2005	230	Control	Volcanic	Drifting plume
V	48	Pagan	11/01/2007	160	Control	Volcanic	Diffuse plume
V	53	Popocatépetl	23/05/2006	250	Control	Volcanic	Interfering signal
V	64	SHV	08/01/2007	240	Control	Volcanic	Drifting plume
V	67	Soputan	19/04/2005	170	Control	Volcanic	Drifting plume

sion in the M_3 methodology. Implementation of this system on a global grid would allow the identification of drifting plumes in addition to those located directly above the corresponding emitting source. One event (V19; Table 4) was impacted by increased noise in the background classification region, also suppressing the plume SO_2 loading in the M_3 calculation. The final factor preventing the correct identification of a volcanic eruption (V53; Table 4) occurred at Popocatépetl (Mexico), through the masking of a moderate eruption plume when a large SO_2 cloud from another volcano (Soufrière Hills, Montserrat) drifted into the M_1 region, causing an anomalously high background SO_2 mass in the M_3 calculation.

4.2 Optimisation of event classification

We assessed the impact of varying the maximum SO_2 plume mass included in the logistic regression model to investigate whether the use of a threshold SO_2 loading improved the classification capabilities of the model. The volcanic dataset was incrementally filtered to remove a proportion of the data, to identify how this influenced the validation statistics. Each reduced volcanic dataset was incorporated into a logistical regression model with a k-fold validation system; however, the control sample was maintained throughout all of the analyses. The variation in class size produced by the removal of volcanic data actually provides a more accurate representation of the natural system (Oommen et al., 2011), with more control samples than volcanic, as more days are characterised by quiescence than volcanic activity. In each instance the overall accuracy, precision, and recall statistics were tracked (Fig. 3) to assess the changes in the model as the minimum incorporated SO_2 mass varied. The linear correlation between control recall and volcanic precision is evident in the comparison of these statistics (Fig. 3b) as well as that between the control precision and volcanic recall.

When all data are incorporated, the model appears to favour volcanic precision and control recall, resulting in a model that will display a larger number of missed volcanic alerts than false classification of control samples. When 60 % of the dataset is used, the volcanic precision and recall are equal, as are the control precision and recall, all displaying values greater than 0.9. The threshold SO_2 loading in this case is 360 t; i.e. if this model were to be implemented, any volcanic plume containing less than this amount would not be identified as a volcanic event. The use of 75 % of the volcanic dataset appears to represent a good compromise between variation in the statistics and the elimination of smaller

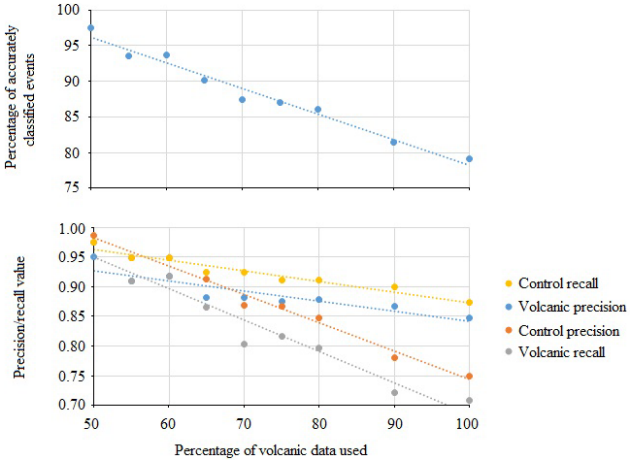

Figure 3. Result of the application of a threshold SO_2 loading to the volcanic dataset on **(a)** accurately classified events and **(b)** the precision (no false alerts) and recall (no missed alerts) values for both the volcanic and control datasets.

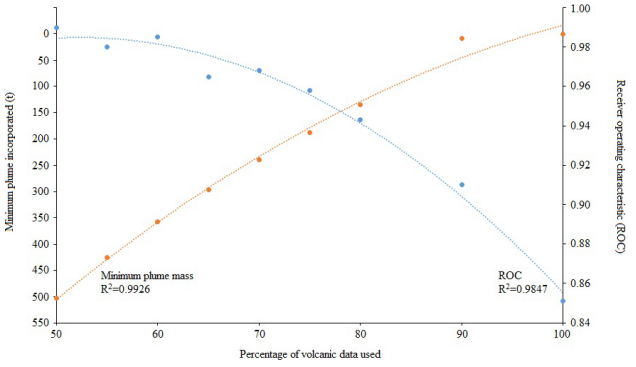

Figure 4. The effect of proportional removal of lowest data points on minimum incorporated SO_2 mass from the volcanic dataset and the ROC (receiver operator characteristic) statistic of each model where ROC = 1 implies all events correctly classified.

plumes (Fig. 3). The volcanic and control precision are almost equal, indicating that this model is equally effective at predicting volcanic and non-volcanic events, with a higher control recall than volcanic recall (Fig. 3). The tendency of this model is to miss smaller volcanic events rather than falsely classify control samples displaying moderate noise levels. Favouring missed over false alerts is also a characteristic of the MODVOLC MODIS-based automatic volcanic alert system (http://modis.higp.hawaii.edu/), designed to detect volcanic thermal anomalies. Quantitative comparison of these models could not be conducted as assessment of the MODVOLC system was performed in a more qualitative manner, assessing whether alerts were identified in locations where they would be expected (e.g. lava flow fields) (Wright et al., 2002, 2004).

Figure 4 shows the variation of ROC values associated with each of the logistic regression models and minimum SO_2 plume mass with the percentage of the total dataset analysed, with the total change in each normalised. The trends in both ROC and SO_2 mass threshold show second-order polynomial characteristics with R^2 values of 0.985 and 0.993 respectively. The intersection of these trend lines represents model optimisation, offering the greatest gain in accuracy (ROC) combined with the least impact on the identifiable SO_2 plume mass. This optimisation point corresponds to the removal of 22 % of the volcanic data, resulting in a minimum incorporated SO_2 mass of $\sim$ 150 t, and correlates with that inferred through the comparison of precision and recall statistics (Fig. 3). Application of a 150 t SO_2 mass threshold prevents the resolution of smaller plumes, but the original assessment (Fig. 2; Table 4) indicates that SO_2 loadings below this value tended to be misclassified anyway.

The model based on 78 % of the volcanic dataset has an overall accuracy of 85.7 % and an ROC of 0.95, producing eight false alerts that correspond to those identified in the original assessment, with the exception of C8 (Table 4), which was accurately classified with this model. In contrast, 27.8% of the missed alerts originally identified were no longer flagged; of these five instances, four were eliminated due to their low SO_2 loadings, with the remaining alert correctly classified as a result of improvements in event classification by the optimised model.

Parameterisation of Eq. (2) using the 78 % model output facilitates the validation of individual records and allows the incorporation of new data points (Eq. 3) through the substitution of X with measured volcanic SO_2 mass in tonnes:

$$P = 1 - \frac{1}{1 + e^{-(-2.943+0.0091X)}}. \quad (3)$$

4.3 Independent validation

A secondary testing procedure was employed to assess the efficacy of the developed logistic regression models on an independent test dataset consisting of 12 volcanic eruptions not initially included (Global Volcanism Program, 2013) and displaying variable plume characteristics, and 12 corresponding control samples, resulting in 24 data points (Table 5).

The incorporation of an independent investigation allowed the data characteristics isolated in the original analysis to be tested against data not utilised in the training of the model. Classification of the data with the original model containing all data points resulted in an accuracy of 75 %, whereas analysis with the optimised model (78 % of the data) produced an overall accuracy of 79.2 %; a detailed overview of the validation statistics of each model is given in Table 6. The optimised model resulted in no false detections although four volcanic events were missed; these consisted of one sample in which the SO_2 plume had drifted out of the analysis area (Soufrière Hills), two weak plumes with SO_2 loadings below 60 t (Cleveland & Lascar), and one moderate plume with SO_2 loadings of 255 t (Colima). All SO_2 plumes exceeding

Table 5. Locations and dates of volcanic and control "eruptions" for validation dataset.

Volcano	Location	Eruption date	Correct classification (Y/N)		Control date	Correct classification (Y/N)	
		(DD/MM/YYY)	Original	Optimised	(DD/MM/YYY)	Original	Optimised
Ambrym	Vanuatu	01/05/2007	N	Y	12/12/2008	N	Y
Anatahan	Mariana Islands	29/05/2006	Y	Y	06/09/2005	Y	Y
Cleveland	Aleutian	06/02/2006	Y	Y	17/05/2009	Y	Y
	Islands	23/05/2006	Y	Y	06/01/2008	Y	Y
		28/10/2006	N	N	28/02/2006	N	N
Colima	Mexico	24/04/2005	N	N	04/05/2009	Y	Y
Lascar	Chile	04/05/2005	N	N	11/02/2007	Y	Y
Lopevi	Vanuatu	21/04/2007	Y	Y	13/12/2006	Y	Y
Okmok	Aleutian Islands	12/07/2008	Y	Y	01/07/2008	Y	Y
Sierra Negra	Galápagos Islands	22/10/2005	Y	Y	04/08/2005	Y	Y
Soputan	Indonesia	25/10/2007	Y	Y	02/07/2008	Y	Y
Soufrière Hills	Montserrat	20/05/2006	N	N	24/08/2006	Y	Y

Table 6. Validation statistics generated through the assessment of the test data with three methods.

Validation statistic	Original model	Optimised model	Optimised threshold model
Overall accuracy (%)	75	79.2	95
Volcanic precision	0.8	1	1
Volcanic recall	0.667	0.583	0.889
Control precision	0.714	0.706	0.917
Control recall	0.833	1	1
ROC	0.813	0.84	0.979
Threshold (P)	0.432	0.620	0.660

390 t were correctly classified as volcanic; therefore we conclude that events emitting less than 390 t SO_2 are likely to be misclassified with this methodology. Taking into account the thresholds of the incorporated methods (Table 6) and solving Eq. (3), we find that the minimum SO_2 mass that would be classified as volcanic in origin by this model is 378 t.

4.4 Limitations

This analysis has indicated that, prior to implementation of the incorporated classification technique (logistic regression), pre-screening of data samples is required to account for the influence of missing data points and meteorological cloud cover. The incorporated modelling technique automatically interpreted missing values as volcanic alerts, thus influencing the calculated threshold, and therefore data gaps must be removed prior to logistic regression analysis. Persistent meteorological cloud cover can mask SO_2 plumes at lower altitudes from satellite sensors, precluding detection. This effect can be significant at higher latitudes, particularly in winter, and therefore the methodology described here may be limited at these locations. Where high-latitude data were available and incorporated into this trial (Bezymianny, Okmok, and Cleveland), correct classification occurred on all but one of those days for which data were available (one additional control sample characterised by no available data was misclassified). Consistent high-latitude classification indicates the robust nature of the M_3 pre-processing technique employed, with no indication that differences in sample region size due to latitudinal variations (discussed in Sect. 2.2) influenced the identification of volcanic clouds. Further investigation is necessary to accurately assess the capabilities of the technique in high-latitude regions, particularly regarding the influence of persistent cloud cover.

The main constraint on SO_2 plume detection using this methodology is the detection limit of the satellite measurements used as input (here, the OMI TRL SO_2 columns). Indeed, this analysis indicates that the minimum SO_2 mass that could be reliably classified as volcanic in origin using the OMI TRL SO_2 data is on the order of 400 t. The lack of a priori knowledge of volcanic SO_2 plume altitude restricts the classification technique to SO_2 retrievals corresponding to a single CMA, and our use of the TRL SO_2 product does not imply any knowledge of SO_2 altitude (which is not required for eruption detection). The use of OMI SO_2 products with lower noise (e.g. STL columns) or more sensitive SO_2 algorithms (e.g. Li et al., 2013) would result in lower detection limits, although STL retrievals would also inhibit the detection of low-altitude or diffuse plumes. Future UV satellite instruments such as the Tropospheric Monitoring Instrument (TROPOMI; http://www.tropomi.eu/), with better spatial resolution than OMI, should also have lower SO_2 detection limits. In order to resolve smaller plumes, an instrument with a higher spatial resolution would be required, but such instruments typically offer lower temporal resolution. Reduced temporal resolution would not provide the daily coverage necessary for the implementation of this technique in a global near-real-time alert system.

Although the technique described here was designed for global detection of volcanic eruptions, it could also be adapted for regional-scale assessments. For initial investigative purposes and model training the location of analysis regions was fixed based upon the location of the known emitting source, although this method could also be implemented on a global or regional scale using a reference grid. Implementation of a gridded analysis over a wider area with the developed analysis performed within each grid cell could allow the classification both above the volcano and in adjacent regions into which plumes may have drifted. For volcanoes with frequent activity during the OMI mission (2004–present), the developed method of data collection and model training could be applied. Application to a single or small cluster of volcanoes would specifically tailor the resulting output to the eruptive style of the volcano or volcanoes in question and could allow refinement of the background correction based on local conditions (e.g. avoiding other known regional SO_2 sources). High frequencies of eruptions and emissions in locations such as Vanuatu or Indonesia could facilitate the training of the data and might prove effective in the monitoring of persistently degassing volcanoes.

5 Conclusions

Through the analysis of operational OMI SO_2 measurements (TRL SO_2 columns) for 79 volcanic eruptions, a simple logistic regression model allowed classification of volcanic from non-volcanic control events with an accuracy of 80 %. Optimisation of the model by progressive removal of input data enabled volcanic plumes containing at least ~ 400 t of SO_2 to be consistently resolved and correctly classified. With an appropriate training dataset, this technique could form the basis of a near-real-time volcanic eruption detection scheme, with minimal user input necessary.

We identified some common factors resulting in misclassification of control or volcanic events, including contamination of the background analysis region with SO_2 emissions from another volcano, low SO_2 emissions and/or low plume altitude (i.e. resulting in emissions below detection limits), advection of SO_2 emissions out of the analysis region prior to the satellite overpass, and data gaps.

The implementation of a NRT volcanic eruption alert system based on the technique described here would represent an advance in small eruption identification over current systems, such as SACS, which use a simple threshold SO_2 column amount to identify significant volcanic degassing events (Brenot et al., 2014). In dispersed volcanic clouds, SO_2 column amounts may be low, yet the total SO_2 loading could be high; hence alerts based on SO_2 mass rather than column amount may be more effective in certain situations. Development of this technique within a global or regional grid system would be effective at identifying drifting volcanic clouds far from the source, which is a current limitation. A combination of both the developed technique and existing SO_2 threshold approaches would likely yield an optimal NRT volcanic cloud detection system suitable for both large drifting plumes and smaller eruptions.

6 Data availability

OMI Level 2 total column SO_2 (OMSO2) data are publicly available from NASA Goddard Earth Sciences Data and Information Services Center (NASA GES DISC, 2016; http://disc.sci.gsfc.nasa.gov/Aura/data-holdings/OMI/omso2_v003.shtml). The OMI processing code used to analyse this data (OMIplot) is available from the Vhub (2016) website (https://vhub.org/resources/682).

Acknowledgements. We acknowledge NASA for supporting this work through the Aura Science Team project (grant NNX11AF42G to Simon A. Carn) and an Earth and Space Science Fellowship to Verity J. B. Flower (NNX14AK94H).

Edited by: B. N. Duncan
Reviewed by: two anonymous referees

References

Brenot, H., Theys, N., Clarisse, L., van Geffen, J., van Gent, J., Van Roozendael, M., van der A, R., Hurtmans, D., Coheur, P.-F., Clerbaux, C., Valks, P., Hedelt, P., Prata, F., Rasson, O., Sievers, K., and Zehner, C.: Support to Aviation Control Service (SACS): an online service for near-real-time satellite monitoring of volcanic plumes, Nat. Hazards Earth Syst. Sci., 14, 1099–1123, doi:10.5194/nhess-14-1099-2014, 2014.

Carn, S. A. and Prata, F. J.: Satellite-based constraints on explosive SO_2 release from Soufrière Hills Volcano, Montserrat, Geophys. Res. Lett., 37, doi:10.1029/2010GL044971, 2010.

Carn, S. A., Krueger, A. J., Bluth, G. J. S., Schaefer, S. J., Krotkov, N. A., Watson, I. M., and Datta, S.: Volcanic eruption detection by the Total Ozone Mapping Spectrometer (TOMS) instruments: A 22-year record of sulphur dioxide and ash emissions, Geological Society, London, Special Publications, 213, 177–202, 2003.

Carn, S. A., Krueger, A. J., Krotkov, N. A., Yang, K., and Levelt, P. F.: Sulfur dioxide emissions from Peruvian copper smelters detected by the Ozone Monitoring Instrument, Geophys. Res. Lett., 34, doi:10.1029/2006GL029020, 2007.

Carn, S. A., Krueger, A. J., Krotkov, N. A., Arellano, S., and Yang, K.: Daily monitoring of Ecuadorian volcanic degassing from space, J. Volcanol. Geotherm. Res., 176, 141–150, doi:10.1016/j.jvolgeores.2008.01.029, 2008.

Carn, S. A., Krotkov, N. A., Yang, K., and Krueger, A. J.: Measuring global volcanic degassing with the Ozone Monitoring Instrument (OMI), Geological Society, London, Special Publications, 380, 229–257, doi:10.1144/SP380.12, 2013.

Carn, S. A., Clarisse, L., and Prata, A. J.: Multi-decadal satellite measurements of global volcanic degassing, J. Volcanol. Geotherm. Res., 311, 99–134, doi:10.1016/j.jvolgeores.2016.01.002, 2016.

Delmelle, P., Stix, J., Baxter, P., Garcia-Alvarez, J., and Barquero, J.: Atmospheric dispersion, environmental effects and potential health hazard associated with the low-altitude gas plume of Masaya volcano, Nicaragua, B. Volcanol., 64, 423–434, 2002.

Fioletov, V. E., McLinden, C. A., Krotkov, N., Moran, M. D., and Yang, K.: Estimation of SO_2 emissions using OMI retrievals, Geophys. Res. Lett., 38, L21811, doi:10.1029/2011GL049402, 2011.

Fioletov, V. E., McLinden, C. A., Krotkov, N., Yang, K., Loyola, D. G., Valks, P., Theys, N., Van Roozendael, M., Nowlan, C. R., Chance, K., and Liu, X: Application of OMI, SCIAMACHY, and GOME-2 satellite SO_2 retrievals for detection of large emission sources, J. Geophys. Res.-Atmos., 118, 11399–11418, doi:10.1002/jgrd.50826, 2013.

Flower, V. J. B., Carn, S. A., and Wright, R.: Impacts of sensor viewing geometry on time-series analysis of volcanic emissions, Remote Sens. Environ., 183, 282–293, doi:10.1016/j.rse.2016.05.022, 2016.

Global Volcanism Program: Volcanoes of the World, v. 4.4.3, edited by: Venzke, E., Smithsonian Institution, doi:10.5479/si.GVP.VOTW4-2013 (last access: 11 June 2016), 2013.

Haahr, M.: Random.org: True random number service, School of Computer Science and Statistics, Trinity College, Dublin, Ireland, available at: http://www.random.org, last access: June, 2015.

Hall, M., Frank, E., Holmes, G., Pfahringer, B., Reutemann, P., and Witten, I. H.: The WEKA data mining software: an update, ACM SIGKDD Explorations newsletter, 11, 10–18, 2009.

Hansell, A. und Oppenheimer, C.: Health hazards from volcanic gases: a systematic literature review, Arch. Environ. Health, 59, 628–639, 2004.

Krotkov, N. A., Carn, S. A., Krueger, A. J., Bhartia, P. K., and Yang, K.: Band residual difference algorithm for retrieval of SO_2 from the Aura Ozone Monitoring Instrument (OMI), IEEE T. Geosci. Remote, 44, 1259–1266, 2006.

Krotkov, N. A., Schoeberl, M. R., Morris, G. A., Carn, S. A., and Yang, K.: Dispersion and lifetime of the SO_2 cloud from the August 2008 Kasatochi eruption, J. Geophys. Res., 115, D00L20, doi:10.1029/2010JD013984, 2010.

Krueger, A. J.: Sighting of El Chichon sulfur dioxide clouds with the Nimbus 7 total ozone mapping spectrometer, Science, 220, 1377–1379, 1983.

Krueger, A., Krotkov, N., and Carn, S.: El Chichon: The genesis of volcanic sulfur dioxide monitoring from space, J. Volcanol. Geoth. Res., 175, 408–414, 2008.

Li, C., Joiner, J., Krotkov, N. A., and Bhartia, P. K.: A fast and sensitive new satellite SO_2 retrieval algorithm based on principal component analysis: Application to the ozone monitoring instrument, Geophys. Res. Lett., 40, 6314–6318, doi:10.1002/2013GL058134, 2013.

Lopez, T., Carn, S., Werner, C., Fee, D., Kelly, P., Doukas, M., Pfeffer, M., Webley, P., Cahill, C., and Schneider, D.: Evaluation of Redoubt Volcano's sulfur dioxide emissions by the Ozone Monitoring Instrument, J. Volcanol. Geoth. Res., 259, 290–307, 2013.

McCormick, B. T., Edmonds, M., Mather, T. A., and Carn, S. A.: First synoptic analysis of volcanic degassing in Papua New Guinea, Geochem. Geophy. Geosy., 13, Q03008, doi:10.1029/2011GC003945, 2012.

McCormick, B. T., Edmonds, M., Mather, T. A., Campion, R., Hayer, C. S., Thomas, H. E., and Carn, S. A.: Volcano monitoring applications of the Ozone Monitoring Instrument, Geological Society, London, Special Publications, 380, 259–291, 2013.

Miller, T. P. and Casadevall, T. J.: Volcanic ash hazards to aviation, Enc. Volcanoes, Academic Press, London, UK, 915–930, 2000.

Murphy, S. W., de Souza Filho, C. R., and Oppenheimer, C.: Monitoring volcanic thermal anomalies from space: Size matters, J. Volcanol. Geoth. Res., 203, 48–61, 2011.

NASA GES DISC: OMI Level 2 total column SO_2 data, available at: http://disc.sci.gsfc.nasa.gov/Aura/data-holdings/OMI/omso2_v003.shtml, last access: 10 November 2016.

Prata, A. J.: Satellite detection of hazardous volcanic clouds and the risk to global air traffic, Nat. Hazards, 51, 303–324, 2009.

Oommen, T., Baise, L. G., and Vogel, R.: Validation and application of empirical liquefaction models, J. Geotech. Geoenviron., 136, 1618–1633, 2010.

Oommen, T., Baise, L. G., and Vogel, R. M.: Sampling bias and class imbalance in maximum-likelihood logistic regression, Mat. Geosci., 43, 99–120, 2011.

Rodríguez, J. D., Perez, A., and Lozano, J. A.: Sensitivity analysis of k-fold cross validation in prediction error estimation, IEEE T. Pattern. Anal., 32, 569–575, 2010.

Schneider, D. J., Dean, K., Dehn, J., Miller, T., and Kirianov, V. Y.: Monitoring and analyses of volcanic activity using remote sensing data at the Alaska Volcano Observatory: case study for Kamchatka, Russia, December 1997, Geoph. Monog. Series, 65–85, 2000.

Self, S., Zhao, J. X., Holasek, R. E., Torres, R. C., and King, A. J.: The atmospheric impact of the 1991 Mount Pinatubo eruption, US Geological Survey (USGS), 1993.

Telling, J. W, Flower, V. J. B., and Carn, S. A.: A multi-sensor satellite assessment of SO_2 emissions from the 2012–13 eruption of Tolbachik volcano, Kamchatka, J. Volcanol. Geoth. Res., 307, 98–106, doi:10.1016/j.jvolgeores.2015.07.010, 2015.

VHub: OMI processing code, available at: https://vhub.org/resources/682, last access: 10 November 2016.

Witten, I. H. and Frank, E.: Data Mining: Practical machine learning tools and techniques, Morgan Kaufmann, 119–127, 2005.

Wright, R., Flynn, L., Garbeil, H., Harris, A., and Pilger, E.: Automated volcanic eruption detection using MODIS, Remote Sens. Environ., 82, 135–155, 2002.

Wright, R., Flynn, L. P., Garbeil, H., Harris, A. J., and Pilger, E.: MODVOLC: near-real-time thermal monitoring of global volcanism, J. Volcanol. Geoth. Res., 135, 29–49, 2004.

Yang, K., Krotkov, N. A., Kruger, A. J., Carn, S. A., Bhartia, P. K., and Levelt, P. F.: Retrieval of large volcanic SO_2 columns from the Aura Ozone Monitoring Instrument: comparison and limitations, J. Geophys. Res.-Atmos., 112, D24S43, doi:10.1029/2007JD008825, 2007.